JOURNAL OF THE MECHANICAL BEHAVIOR OF BIOMEDICAL MATERIALS 56 (2016) 175–182

Available online at www.sciencedirect.com

ScienceDirect

www.elsevier.com/locate/jmbbm

Research paper

Microrobotized blasting improves the bone-to-textured implant response. A preclinical in vivo biomechanical study

Paulo G. Coelho[a,b,c], *Luiz F. Gil*[d], *Rodrigo Neiva*[e], *Ryo Jimbo*[f], *Nick Tovar*[a], *Thomas Lilin*[g], *Estevam A. Bonfante*[h,*]

[a]*Department of Biomaterials and Biomimetics, New York University, 433 1st Ave., Room 844, New York, NY 10010, USA*
[b]*Director for Research, Department of Periodontology and Implant Dentistry, New York University College of Dentistry, 345E 24th Street, New York, NY 10010, USA*
[c]*Affiliated Faculty, Department of Engineering, New York University Abu Dhabi, PO Box 129188, Abu Dhabi, United Arab Emirates*
[d]*Department of Dentistry, Division of Oral and Maxillofacial Surgery, Universidade Federal de Santa Catarina, R. Eng. Agronômico Andrei Cristian Ferreira, s/n-Trindade, Florianópolis, SC 88040-900, Brazil*
[e]*Department of Periodontology, University of Florida at Gainesville, 1395 Center Dr, Gainesville, FL 32610, USA*
[f]*Department of Prosthodontics, Malmo University, Malmo 205 06, Sweden*
[g]*École Nationale Vétérinaire d'Alfort, 7 Avenue du Général de Gaulle, 94704 Mainsons-Alfort, France*
[h]*Department of Prosthodontics, University of Sao Paulo – Bauru College of Dentistry, Alameda Otávio Pinheiro Brisola 9-75, Bauru, SP 17.012-901, Brazil*

ARTICLE INFO

Article history:
Received 25 August 2015
Received in revised form
6 November 2015
Accepted 9 November 2015
Available online 24 November 2015

Keywords:
Implant
Surface
Bone
Mechanical
Healing chamber
Histology

ABSTRACT

This study evaluated the effect of microrobotized blasting of titanium endosteal implants relative to their manually blasted counterparts. Two different implant systems were utilized presenting two different implant surfaces. Control surfaces (Manual) were fabricated by manually grit blasting the implant surfaces while experimental surfaces (Microblasted) were fabricated through a microrobotized system that provided a one pass grit blasting routine. Both surfaces were created with the same ~50 μm average particle size alumina powder at ~310 KPa. Surfaces were then etched with 37% HCl for 20 min, washed, and packaged through standard industry procedures. The surfaces were characterized through scanning electron microscopy (SEM) and optical interferometry, and were then placed in a beagle dog radius model remaining in vivo for 3 and 6 weeks. The implant removal torque was recorded and statistical analysis evaluated implant system and surface type torque levels as a function of time in vivo. Histologic sections were qualitatively evaluated for tissue response. Electron microscopy depicted textured surfaces for both manual and microblasted surfaces. Optical interferometry showed significantly higher S_a, S_q, values for the microblasted surface and no significant difference for S_{ds} and S_{dr} values between surfaces. In vivo results depicted that statistically significant gains in biomechanical fixation were obtained for both implant systems tested at 6 weeks in vivo,

*Corresponding author. Tel.: +55 14 3235 8277.
E-mail address: estevamab@gmail.com (E.A. Bonfante).

http://dx.doi.org/10.1016/j.jmbbm.2015.11.002
1751-6161/© 2015 Elsevier Ltd. All rights reserved.

while only one system presented significant biomechanical gain at 3 weeks. Histologic sections showed qualitative higher amounts of new bone forming around microblasted implants relative to the manually blasted group. Microrobotized blasting resulted in higher biomechanical fixation of endosteal dental implants and should be considered as an alternative for impant surface manufacturing.

© 2015 Elsevier Ltd. All rights reserved.

1. Introduction

The host to metallic implant response has been extensively studied and through implant system surgical hardware (relationship between implant bulk design and surgical instrumentation dimension) engineering, surface engineering at multiple length scales, and tissue engineering approaches, the host-to-implant response has significantly reduced the time required for the establishment of a biomechanically competent bone-implant interlocking (Coelho et al., 2015).

Although it has been recently shown that alterations in surgical hardware alter the osseointegration pathway of metallic devices (Coelho and Jimbo, 2014), surface engineering has been deemed equally important as an ad-hoc engineering design tool since the implant surface is the first component of the implant to interact with the host biomolecules and thus may modulate tissue and cellular events that may improve/accelerate tissue integration. Such surface engineering techniques have extensively been explored at the micrometer and nanometer scales (Coelho et al., 2015; Johansson et al., 2012), as well as surface coatings with bioactive ceramics (Jimbo et al., 2012). It has been reported that surface modifications promote earlier osseointegration, which has significantly contributed to the transition of the clinical modality. Currently, the majority of commercially available implant surfaces are physically and/or chemically modified and are alleged by industries to promote shorter healing periods. Evidence in the literature also indicates that surface modified implants are beneficial when utilized especially in clinically compromised situations (Khang et al., 2001; Pinholt, 2003; Stach and Kohles, 2003).

To date, continuous research in this field has focused in further enhancement of osseointegration and recent reports showed that the addition of biomolecules provided favorable outcomes (Coelho et al., 2014a', 2014b; Yoo et al., 2014). While promising, tissue engineering approaches are still far from reaching industrial scale due to challenges in product economic viability and large scale industrial surface engineering methods comprise grit blasting the implant surface through methods that provide little control of the process (i.e. manually). This is supposedly one of the reasons why implant surfaces, even within the same manufacturer and type, may vary in roughness depending on their batches. Although these batches all may be within the so-called moderately roughened surface roughness, which is known to present the strongest bone responses (Wennerberg and Albrektsson, 2009), the coarse differences in the surface roughness would result in different biologic outcomes. Due to the fact that cells and proteins respond sensitively to fractional alterations in the surface topography (Cooper, 2000), a slight deviation in surface roughness could result in adverse effects. Valverde et al. (2013) reported that implant surface roughness may be altered by the blasting media size, velocity, and surface coverage and suggested that the controlled blasting procedure could allow tailored surface topographical conditions. The microrobotization of the surface roughening procedure not only standardizes precision of the surface topography but also allows its modification by alteration of multiple parameters.

In this study, we have tested the bone/implant interface biomechanical competence of two different implant systems that were fabricated with the same materials and pressure parameters either manually or through a microrobotized process in a laboratory in vivo model. The objective was to test whether the microrobotized roughening process would present improved osseointegration to the implant surface as compared to the manually treated surfaces. It was hypothesized that the high precision and homogeneity of the microrobotized surface roughening procedure would present higher osteoconductivity compared to the manually blasted controls.

2. Materials and methods

2.1. Materials

Sixty commercially pure grade 2 titanium alloy, threaded endosseous implants were utilized in the study. Half of these implants were control surfaces (Manual) that were fabricated by manually grit blasting while the other half were experimental surfaces (Microblasted) that were fabricated through a miocrorobotized system that provided a one pass grit-blasting routine. For both processes the implants were mounted with customized fixtures in a rotating column. Both surfaces were created with the same ~50 μm average particle size alumina powder at ~310 KPa. Both surfaces were then subjected to a 37% HCl etching procedure for 20 min and were washed and packaged through standard industry procedures. Information regarding both processing parameters are presented in Table 1.

Thirty implants (Duocon System, Signo Vinces, Campo Largo, PR, Brazil) of 3.8 mm diameter by 10 mm length presented a microthreaded cervical component with a large thread pitch along the body of the implant (Fig. 1a). The other thirty implants (Slim System, Signo Vinces, Campo Largo, PR, Brazil) presented dimensions of 3.5 mm diameter by 10 mm length presented with a large thread pitch throughout its

Table 1 – Manual and microblasting processing parameters.

Blasting parameter	Manual	Microblasted
Distance from nozzle	5 mm	1.5 mm
Nozzle angulation	1st Pass: perpendicular to implant long axis, 2nd pass: +45° relativeinitial position, 3rd pass: −45° from initial position	Perpendicular to implant long axis
Implant rotation velocity	220 rpm	105 rpm
Blasting time	~60 s	~20 s

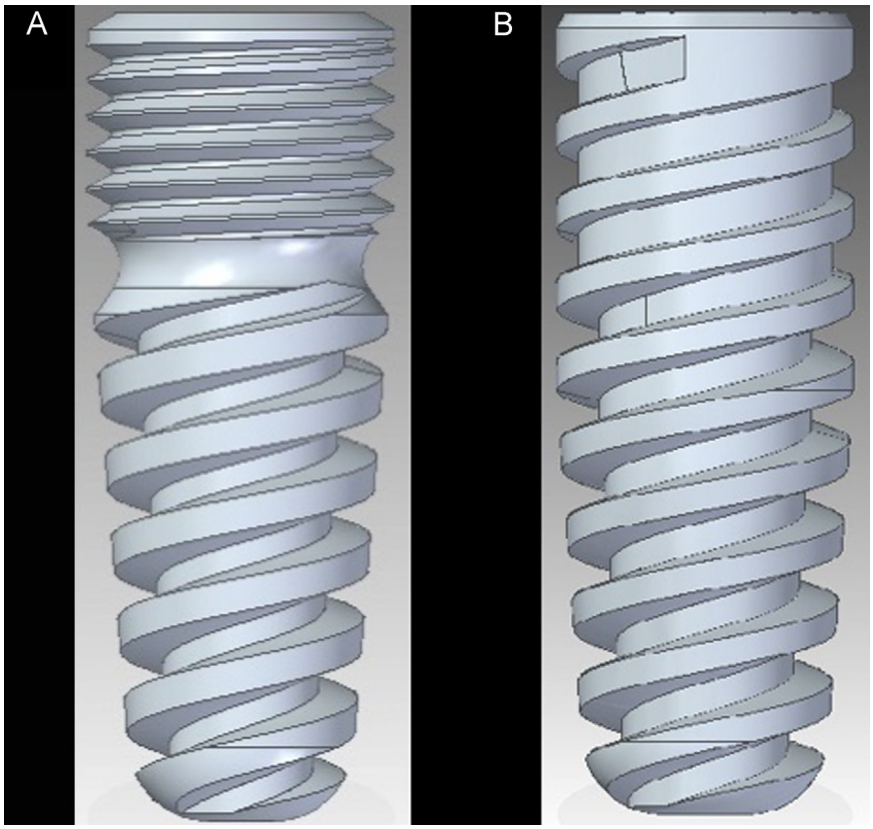

Fig. 1 – (left) the Duocon and the (right) Slim implant geometries.

length from apical to cervical. Three implants of each system and surface were utilized for surface characterization, and twelve implants of each system and surface were utilized in the in vivo animal study.

2.2. *Surface texture characterization*

For surface texture characterization, three implants per surface condition were utilized. Scanning electron microscopy (SEM, Philips XL 30, Eindhoven, The Netherlands) was performed at various magnifications under an acceleration voltage of 15 kV. Verification of particle embedding composition was performed by energy dispersive spectroscopy (EDS) at various accelerating voltages (PGT IMIX with PRISM light element detectors). Surface roughness was evaluated in the different surface implants by optical interferometry (IFM, Phase View 2.5, Palaiseau, France) at the flat region of the implant cutting edges (three measurements per implant). S_a (arithmetic average high deviation), S_q (root mean square), S_{ds} (density of summits), and S_{dr} (developed surface ratio) parameters were determined. A filter size of 250 μm × 250 μm was utilized for a total of 15 measurements per surface of each implant type. IFM parameter statistical analysis was performed by one-way ANOVA. Statistical significance was indicated by p-levels less than 5%.

2.3. *In vivo laboratory model*

For the laboratory in vivo model, 6 adult male beagle dogs approximately 1.5 years old were acquired after the approval of the Ethics Committee for Animal Research at Ecole National Veterinaire D'Alfort.

Prior to general anesthesia, intramuscular atropine sulfate (0.044 mg/kg) and xylazine chlorate (8 mg/kg) were administered. A 15 mg/kg ketamine chlorate dose was then used to achieve general anesthesia.

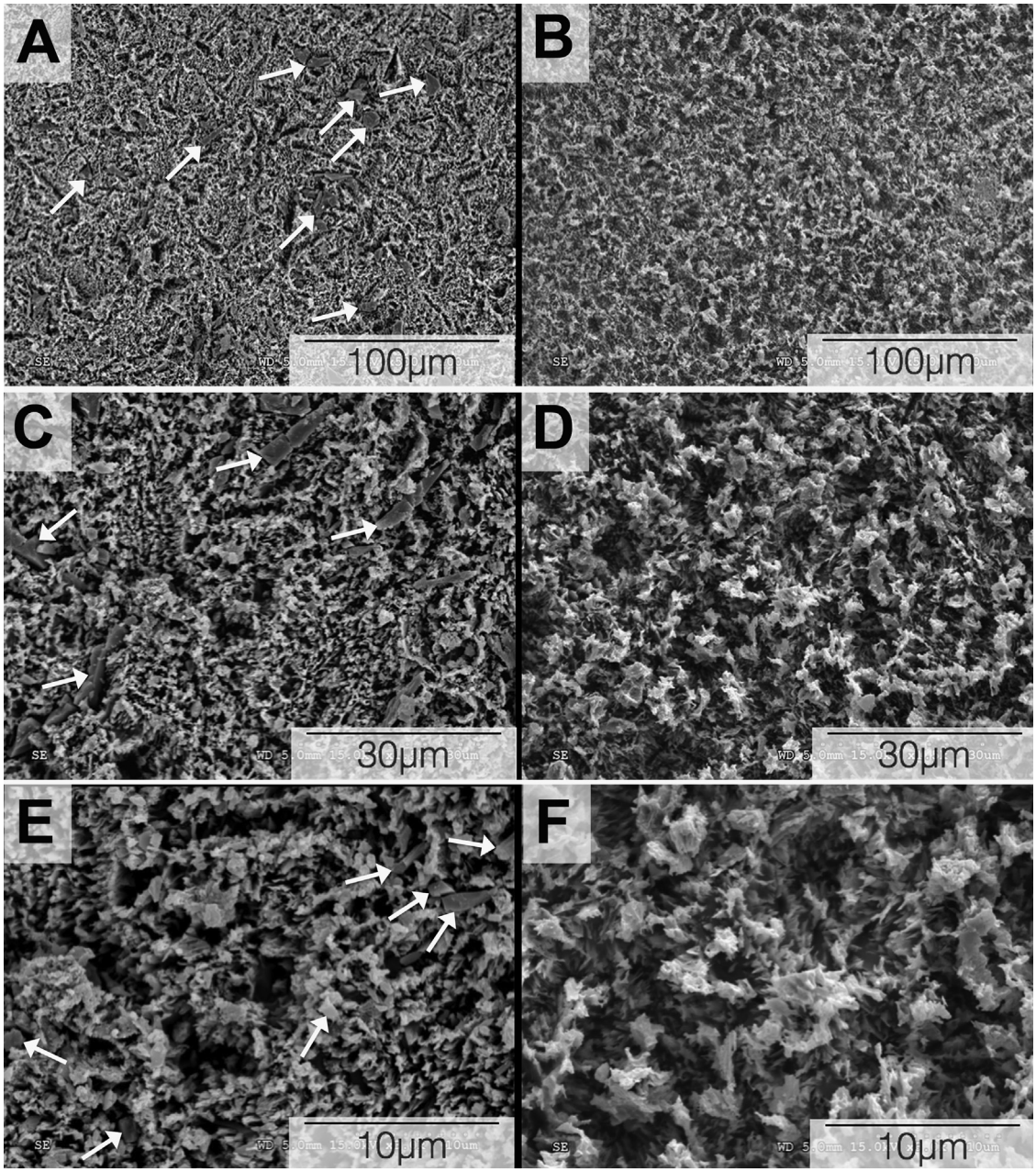

Fig. 2 – Scanning electron micrographs for the (a, c, e) manual and (b, d, f) for the microblasted surfaces at various magnifications. Note the presence of embedded alumina particles for the manual and the absence of particle embedding for the microblasted surface (arrows). Representative micrographs obtained from Duocon implants, similar characteristics were also observed for Slim implants.

The central region of the radius diaphysis was used for the surgery. After hair shaving, skin exposure, and antiseptic cleaning with iodine solution at the surgical and surrounding area, approximately a 5 cm length incision to access the periosteum was performed and a flap was thereafter reflected for bone exposure.

Four implants were placed along the radius from proximal to distal in an alternated distribution of system and surface type in every radius. This approach resulted in balanced surgical procedures that allowed the comparison of the same number of implant surfaces per time in vivo, limb, surgical site (1 through 4), and animal. The implants remained in vivo for either 3 or 6 weeks (right and left radius provided samples that remained in vivo for 3 and 6 weeks, respectively). The implants were placed at distances of 1 cm from each other along the central region of the bone.

After insertion, each implant received its proprietary cover screw to avoid tissue overgrowth. The soft tissue was sutured in layers according to standard procedures, with the periosteum and muscle layers sutured with Vicryl 4-0 (Ethicon, Johnson & Johnson, Miami, FL) and the skin with 4-0 nylon (Ethicon).

Table 2 – IFM measurements for the different surfaces.

	S_a (μm)	S_q (μm)	S_{ds} (summits/mm^2)	S_{dr} (%)
Microblasted	0.66	0.80	4677.50	35.00
Standard dev	0.13	0.17	1290.85	2.90
Manual	0.33	0.42	6433.17	38.67
Standard dev	0.09	0.10	2330.29	5.41
p-values	0.001	0.002	0.21	0.90

Postoperative antibiotic and anti-inflammatory medications included a single dose of benzyl penicillin benzatine (20,000 UI/kg) intramuscularly and ketoprofen 1% (1 ml/5 kg). The dogs were euthanized by an anesthesia overdose, and the limbs were retrieved by sharp dissection. The soft tissue was carefully removed by surgical blade, and an initial clinical evaluation was performed to determine implant stability. If an implant was clinically unstable, it was excluded from the study.

For the torque testing, the radii were adapted to an electronic torque machine equipped with a 250 Ncm torque load cell (Test Resources, Minneapolis, MN, USA). Custom machined tooling was adapted to each implant internal connection and the bone block was carefully positioned to avoid specimen misalignment during testing. The implants were torqued in the counter clockwise direction at a rate of ~0.196 rad/min, and torque to interface fracture was recorded. The torque machine was set to automatically stop the measurement when a torque drop of 10% from the highest recorded torque was detected. The rationale for this procedure was to minimize interface damage prior to histologic procedures, subsequently allowing qualitative histologic assessment. As such, careful biomechanical testing allowed each block to be used for both biomechanical and histologic evaluation (Coelho and Lemons, 2009; Granato et al., 2009, Granato et al., 2011).

The bones were reduced to blocks containing the implants and surrounding bone, and were immersed in 10% buffered formalin solution for 24 h. The blocks were then washed in running water for 24 h, and gradually dehydrated in a series of alcohol solutions ranging from 70% to 100% ethanol. Following dehydration, the samples were embedded in a methacrylate-based resin (Technovit 9100, Heraeus Kulzer GmbH, Wehrheim, Germany) according to the manufacturer's instructions. The blocks were cut into slices (~300 μm thickness) aiming the center of the implant along its long axis with a precision diamond saw (Isomet 2000, Buehler Ltd., Lake Bluff, IL, USA), glued to acrylic plates with an acrylate-based cement, and a 24 h setting time was allowed prior to grinding and polishing. The sections were then reduced to a final thickness of ~30 μm by means of a series of SiC abrasive papers (400, 600, 800, 1200 and 2400) (Buehler Ltd., Lake Bluff, IL, USA) in a grinding/polishing machine (Metaserv 3000, Buehler Ltd., Lake Bluff, IL, USA) under water irrigation (Donath and Breuner, 1982). The sections were then stained by toluidine blue and histomorphologically evaluated with optical microscopy. The histologic samples were evaluated at 50–200 × magnification (Leica DM2500M, Leica Microsystems GmbH, Wetzlar, Germany).

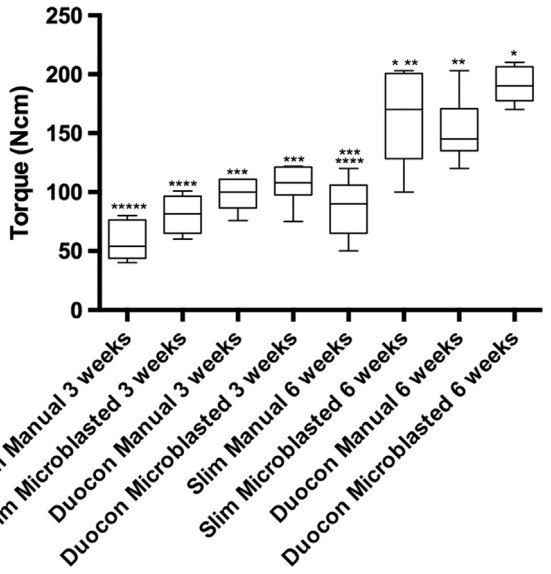

Fig. 3 – Torque to interface fracture for the different implant systems and surfaces as a function of time in vivo. Statistically homogeneous groups present the same number of asterisks.

Preliminary statistical analyses showed no effect of implant site (i.e., there were no consistent effects of positions along the radii) on all measurements. Therefore, site was not considered further in the analysis. Further statistical evaluation of torque at 3 and 6 weeks employed a mixed-model ANOVA where the animal was considered the statistical unit ($n=6$). Statistical significance was indicated by *p*-levels less than 5%, and post-hoc testing employed the Fisher LSD test.

3. Results

Fig. 2 depicts representative scanning electron micrographs for both the manual and microblasted surfaces at different magnifications. From a qualitative perspective, both surfaces presented similar textured morphology (Fig. 2) due to the grit-blasting followed by the acid-etching procedures. Relative to the microblasted surfaces, the manually prepared implant surfaces presented evidence of alumina particles embedded within the textured titanium surface.

Table 2 presents the S_a, S_q, S_{ds}, and S_{dr} mean and standard deviations, as well as the *p* values obtained for the different surfaces' comparisons. Significant differences favoring the microblasted surface were detected in the S_a and S_q values and no differences were observed in S_{ds} and S_{dr} values (Table 2).

The removal torque statistical summary is presented in Fig. 3. At 3 weeks, increased levels of removal torque were observed for both implant systems with the microblasted surface relative to the control. However, statistical significance was only reached for the Slim system ($p<0.02$). At 6 weeks, the microblasted surface condition in both implant systems presented significantly higher removal torque values ($p<0.01$) (Fig. 3).

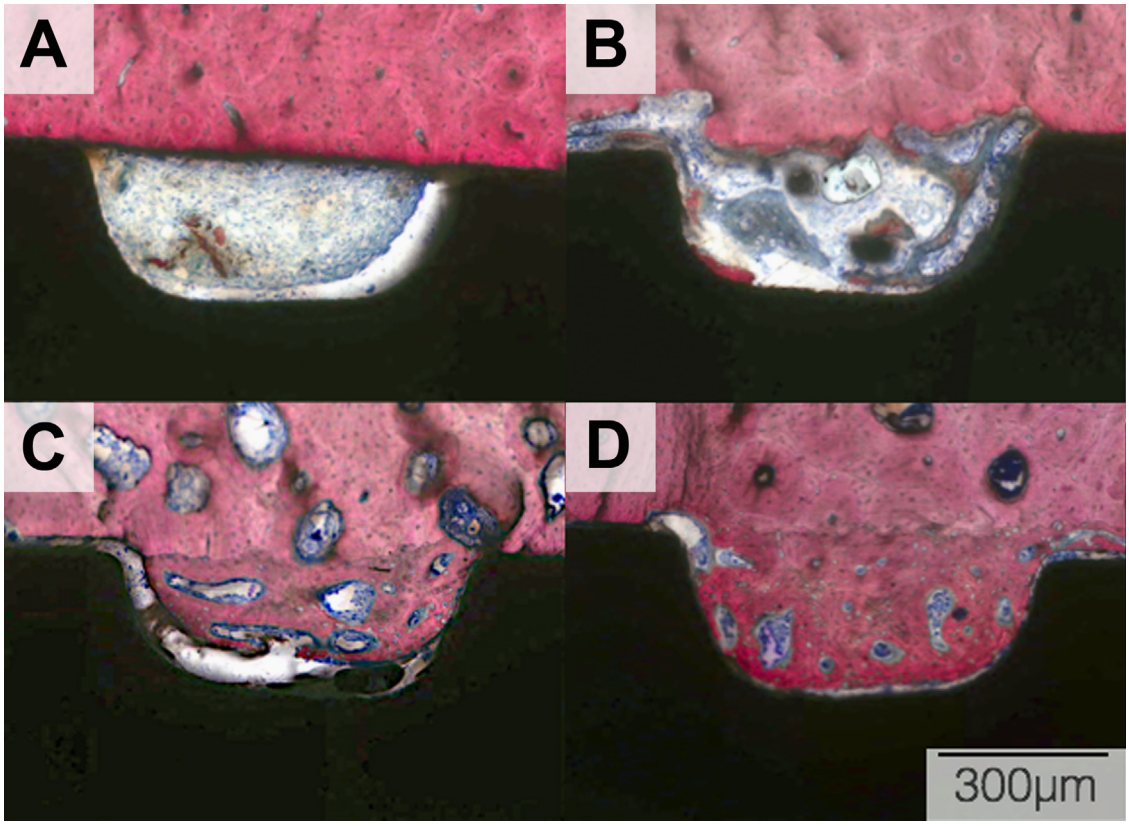

Fig. 4 – At 3 weeks, (a) manual and (b) microblasted surface implants presented a healing chamber filled with osteogenic tissue where initial bone formation observed in higher amounts for the microblasted surface relative to its manually blasted counterpart. At 6 weeks, (c) manual and (d) microblasted surface implants presented high degrees of bone filling relative to three weeks. The gaps observed in the micrographs between tissue and implant were likely generated by the mechanical testing performed prior to histologic sectioning. Representative micrographs of the Slim implant.

Qualitative histologic sections depicted that healing chambers were formed along the body of both implant systems due to their macrogeometry and surgical instrumentation dimensions geometric relationship. At 3 weeks, an osteogenic tissue typical of intramembranous-like bone healing pathway was observed occupying the healing chambers for both the manually blasted (Fig. 4a) and microblasted (Fig. 4b) surfaces. However, higher degrees of bone formation and osteoid were observed for the microblasted surfaces relative to their manually blasted counterparts. At 6 weeks, the healing chambers presented substantially more bone filling relative to three weeks (Fig. 4c–d).

4. Discussion

This study observed the effect of microrobotized surface blasting procedures on osseointegration. Implant surfaces that were treated manually with the same setups were considered as controls. Although treated with the same aluminum oxide (alumina) particles and similar parameters, the results of the surface topographical measurements clearly indicated that the 2 blasting procedures generated 2 different surfaces. It was evident from the amplitude parameters that implant surfaces treated by the microblasted (microrobotized) procedure resulted in significantly higher S_a and S_q values than that of the manually blasted procedure. Morphologically, remnants of the alumina particles could evidently be captured with the SEM, whereas the surface for the microblasted group presented a homogeneous morphology. Apparently, these differences resulted in higher osteogenic responses to the implant surface for the microblasted implant group compared to the manually blasted implant group. Specifically, the removal torque (RTQ) values were significantly higher for both implant types at 6 weeks for the microblasted surfaces and at 3 weeks, the RTQ values were significantly higher for one implant type (Duocon) with microblasting and for the Slim group the mean values were higher for the microblasted group (no statistical difference). These results suggested that osteogenic cells sensitively responded to the rougher and homogeneous microstructures, however at the same time, suggested that the interplay between the macrogeometry is of some importance. The macrogeometry of the Slim group generates a healing chamber situation between the implant and the wall of the osteotomy for the entire length of the implant even at the cortical regions, where for the Duocon group, the neck (microthreaded) portion was engaged in a press-fit situation. These differences may have resulted in the biologic differences since the healing chamber situation has been suggested to promote rapid osteoconduction due to the intramembranous-like healing pathway (Coelho and Jimbo, 2014).

The reason why remnants of alumina were evident on the manually blasted surface remain largely speculative, however, the irregular blasting patterns of the manual blasting procedure may have generated more embedding of the alumina particles. Although the negative chemical effect on the bone formation by the residual alumina has been discarded in some studies (Piattelli, 2003; Wennerberg et al., 1996a; Wennerberg et al., 1996b), some other studies indicate that Al ions that may be released in the vicinity of the implant interface, which may inhibit normal bone deposition and mineralization (Capdevielle et al., 1998; Stea et al., 1992; Thompson and Puleo, 1996). However, in clinical reality, the commercially available implants, which possess alumina particles on their surfaces have successfully been in function for decades (Jimbo and Albrektsson, 2015; Pjetursson et al., 2012). Within the current existing evidence, it can be suggested that the effect of the remaining alumina on the implant surface may have had some influence, however, not to the extent that the effects could be considered negative. Hypothetically, the promotion of osseointegration was mainly due to the effect of the successful surface roughening procedure, which was nearly 150% of an increase in average roughness and root square mean roughness.

In this study, microblasting the implant surface significantly promoted the biomechanical stability of the implants placed in the beagle dog model after 3 and 6 weeks in vivo. It would be of interest to investigate whether the effect of a controlled surface blasting procedure influences extended healing periods.

Acknowledgments

To Conselho Nacional de Desenvolvimento Científico e Tecnológico (CNPq), Grant #309475/2014-7

REFERENCES

Capdevielle, M.C., Hart, L.E., Goff, J., Scanes, C.G., 1998. Aluminum and acid effects on calcium and phosphorus metabolism in young growing chickens (*Gallus gallus domesticus*) and mallard ducks (*Anas platyrhynchos*). Arch. Env. Contam. Toxicol. 35, 82–88.

Coelho, P.G., Jimbo, R., 2014. Osseointegration of metallic devices: current trends based on implant hardware design. Arch. Biochem. Biophys. 561, 99–108.

Coelho, P.G., Jimbo, R., Tovar, N., Bonfante, E.A., 2015. Osseointegration: hierarchical designing encompassing the macrometer, micrometer, and nanometer length scales. Dent. Mater. 31, 37–52.

Coelho, P.G., Teixeira, H.S., Marin, C., Witek, L., Tovar, N., Janal, M.N., Jimbo, R., 2014a. The in vivo effect of P-15 coating on early osseointegration. J. Biomed. Mater. Res. B Appl. Biomater. 102, 430–440.

Coelho, P.G., Teixeira, H.S., Marin, C., Witek, L., Tovar, N., Janal, M. N., Jimbo, R., 2014b. The in vivo effect of P-15 coating on early osseointegration. J. Biomed. Mater. Res. B: Appl. Biomater. 102, 430–440.

Coelho, P.G., Lemons, J.E., 2009. Physico/chemical characterization and in vivo evaluation of nanothickness bioceramic depositions on alumina-blasted/acid-etched Ti-6Al-4V implant surfaces. J. Biomed. Mater. Res. A. 90 (2), 351–361, http://dx.doi.org/10.1002/jbm.a.32097.

Cooper, L.F., 2000. A role for surface topography in creating and maintaining bone at titanium endosseous implants. J. Prosthet. Dent. 84, 522–534.

Donath, K., Breuner, G., 1982. A method for the study of undecalci- fied bones and teeth with attached soft tissues. The Sage– Schliff (sawing and grinding) technique. J. Oral Pathol. 11, 318–326.

Granato, R., Marin, C., Suzuki, M., Gil, J.N., Janal, M.N., Coelho, P. G., 2009. Biomechanical and histomorphometric evaluation of a thin ion beam bioceramic deposition on plateau root form implants: an experimental study in dogs. J Biomed. Mater. Res. B. Appl. Biomater 90 (1), 396–403, http://dx.doi.org/10.1002/jbm.b.31298.

Granato, R., Marin, C., Gil, J.N., Chuang, S.K., Dodson, T.B., Suzuki, M., Coelho, P.G., 2011. Thin bioactive ceramic-coated alumina-blasted/acid-etched implant surface enhances biomechanical fixation of implants: an experimental study in dogs. Clin. Implant Dent. Relat. Res 13 (2), 87–94, http://dx.doi.org/10.1111/j.1708-8208.2009.00186.x.

Jimbo, R., Albrektsson, T., 2015. Long-term clinical success of minimally and moderately rough oral implants: a review of 71 studies with 5 years or more of follow-up. Implant. Dent. 24, 62–69.

Jimbo, R., Coelho, P.G., Bryington, M., Baldassarri, M., Tovar, N., Currie, F., Hayashi, M., Janal, M.N., Andersson, M., Ono, D., Vandeweghe, S., Wennerberg, A., 2012. Nano hydroxyapatite-coated implants improve bone nanomechanical properties. J. Dent. Res. 91, 1172–1177.

Johansson, C.B., Gretzer, C., Jimbo, R., Mattisson, I., Ahlberg, E., 2012. Enhanced implant integration with hierarchically structured implants: a pilot study in rabbits. Clin. Oral. Implant. Res. 23, 943–953.

Khang, W., Feldman, S., Hawley, C.E., Gunsolley, J., 2001. A multicenter study comparing dual acid-etched and machined-surfaced implants in various bone qualities. J. Periodontol. 72, 1384–1390.

Piattelli, A., 2003. Residual aluminum oxide on the surface of titanium implants has no effect on osseointegration. Biomaterials 24, 4081–4089.

Pinholt, E.M., 2003. Branemark and ITI dental implants in the human bone-grafted maxilla: a comparative evaluation. Clin. Oral Implant. Res. 14, 584–592.

Pjetursson, B.E., Thoma, D., Jung, R., Zwahlen, M., Zembic, A., 2012. A systematic review of the survival and complication rates of implant-supported fixed dental prostheses (FDPs) after a mean observation period of at least 5 years. Clin. Oral Implant. Res. 23, 22–38.

Stach, R.M., Kohles, S.S., 2003. A meta-analysis examining the clinical survivability of machined-surfaced and osseotite implants in poor-quality bone. Implant. Dent. 12, 87–96.

Stea, S., Savarino, L., Toni, A., Sudanese, A., Giunti, A., Pizzoferrato, A., 1992. Microradiographic and histochemical evaluation of mineralization inhibition at the bone-alumina interface. Biomaterials 13, 664–667.

Thompson, G.J., Puleo, D.A., 1996. Ti–6Al–4V ion solution inhibition of osteogenic cell phenotype as a function of differentiation timecourse in vitro. Biomaterials 17, 1949–1954.

Valverde, G.B., Jimbo, R., Teixeira, H.S., Bonfante, E.A., Janal, M.N., Coelho, P.G., 2013. Evaluation of surface roughness as a function of multiple blasting processing variables. Clin. Oral Implant. Res. 24, 238–242.

Wennerberg, A., Albrektsson, T., 2009. Effects of titanium surface topography on bone integration: a systematic review. Clin. Oral Implant. Res. 20 (Suppl 4), S172–S184.

Wennerberg, A., Albrektsson, T., Johansson, C., Andersson, B., 1996a. Experimental study of turned and grit-blasted screw-

shaped implants with special emphasis on effects of blasting material and surface topography. Biomaterials 17, 15–22.

Wennerberg, A., Albrektsson, T., Lausmaa, J., 1996b. Torque and histomorphometric evaluation of c.p. titanium screws blasted with 25- and 75-microns-sized particles of Al_2O_3. J. Biomed. Mater. Res. 30, 251–260.

Yoo, D., Tovar, N., Jimbo, R., Marin, C., Anchieta, R.B., Machado, L. S., Montclare, J., Guastaldi, F.P.S., Janal, M.N., Coelho, P.G., 2014. Increased osseointegration effect of bone morphogenetic protein 2 on dental implants: Anin vivostudy. J. Biomed. Mater. Res. A 102, 1921–1927.